Short Papers

Tracking Nonrigid Motion and Structure from 2D Satellite Cloud Images without Correspondences

Lin Zhou, Chandra Kambhamettu, *Member*, *IEEE*,
Dmitry B. Goldgof, *Sr. Member*, *IEEE*,
K. Palaniappan, *Sr. Member*, *IEEE*,
and A.F. Hasler

Abstract—Tracking both structure and motion of nonrigid objects from monocular images is an important problem in vision. In this paper, a hierarchical method which integrates local analysis (that recovers small details) and global analysis (that appropriately limits possible nonrigid behaviors) is developed to recover dense depth values and nonrigid motion from a sequence of 2D satellite cloud images without any prior knowledge of point correspondences. This problem is challenging not only due to the absence of correspondence information but also due to the lack of depth cues in the 2D cloud images (scaled orthographic projection). In our method, the cloud images are segmented into several small regions and local analysis is performed for each region. A recursive algorithm is proposed to integrate local analysis with appropriate global fluid model constraints, based on which a structure and motion analysis system, SMAS, is developed. We believe that this is the first reported system in estimating dense structure and nonrigid motion under scaled orthographic views using fluid model constraints. Experiments on cloud image sequences captured by meteorological satellites (GOES-8 and GOES-9) have been performed using our system, along with their validation and analyses. Both structure and 3D motion correspondences are estimated to subpixel accuracy. Our results are very encouraging and have many potential applications in earth and space sciences, especially in cloud models for weather prediction.

Index Terms—Nonrigid objects, structure estimation, image motion estimation, fluid models.

1 Introduction

Cloud motion analysis is a very important application area in computer vision, especially in nonrigid motion analysis. Accurate cloud heights and winds are significant for a number of meteorological and climate applications [7], such as cloud model verification, physically-based numerical weather prediction and data assimilation, cloud-wind height assignment [6], [8], [18], [7], convective intensity estimation [24], [25], naval aviation, and radiation balance estimation for Mission to Planet Earth type climate baseline studies.

During the past decades, many studies have been conducted on the structure recovery from rigid motion [30], [2] and the motion recovery from stereo images [32]. In particular, different vision algorithms were proposed and employed to address the problem of automatic cloud motion analysis. Fujita et al. pioneered the use of ATS-1, the first geosynchronous meteorological satellites, launched in 1966, for measuring large scale cloud motion [5]. Leese et al. [16], Smith and Phillips [26], and Phillips et al. [23] implemented local area cross-correlation-based automatic cloud tracking using ATS imagery. Cross-correlation methods implicitly assume a local rigid motion model. However, this assumption fails in tracking mesoscale atmospheric phenomena such as hurricanes and severe convective storms [9]. Aggarwal and Duda [1] studied the motion of polygonal objects and used vertices as matching features to estimate cloud motions from satellite images. Kambhamettu et al. [14] used a *continuous motion model*, where individual cloud elements are assumed to undergo locally continuous deformation (i.e., the cloud surface patch can be smoothly stretched with local elements maintaining their neighborhood relationships), while Palaniappan et al. [20], [19] used a *semifluid model* which allows cloud surface patches to merge, split, or cross over. However, their methods relied on 3D cloud data and utilized the changes in differential geometric properties of 3D cloud surfaces in motion in order to perform cloud tracking. The 3D cloud data were obtained from stereo analysis and/or by approximating 2D intensity images for depth information. Kambhamettu et al. [12] applied coupled stereo and motion analysis of clouds using a simple-to-complex multiresolution approach. Recently, multispectral satellite information, such as moisture data and infrared data, was incorporated into the automatic cloud motion vector estimation algorithms by Velden [27] and Velden et al. [28], [29]. They discussed the impact of multispectral satellite information on both tropical cyclone tracking and cloud intensification analysis.

The previous approaches focused on dense nonrigid motion estimation of clouds using multiview or multispectral satellite cloud image sequences. However, they did not recover dense structure and nonrigid motion from a single 2D image sequence. In this paper, we generalize our previous work in [34], [35] and propose a novel algorithm to estimate both dense structure and nonrigid motion from a sequence of 2D cloud images using global fluid model constraints. The task is challenging due to the complex dynamics of the imaging instruments and the underlying nonlinear phenomena of cloud formation and weather, as well as the scaled orthographic projection of cloud imagery, which makes the structure estimation problem even more difficult. In our algorithm, the cloud images are first segmented into small regions and local analysis is performed for each region, assuming that similar nonrigid motion is present within each region for a short time period. Then, a recursive algorithm is proposed to integrate local analysis with appropriate global constraints. A system called SMAS has been implemented based on our algorithm. Experiments using Hurricane Luis image sequences were performed to estimate the complete hurricane structure and 3D motion correspondences, along with extensive error analysis. The remainder of this paper is organized as follows: Section 2 explains the data acquisition of cloud image sequences. Section 3 briefly presents the local analysis of 2D cloud image sequences. Section 4 discusses the global analysis. Section 5 presents the experimental results on satellite images of Hurricane Luis. Section 6 validates and evaluates our results. Finally, conclusions and future work are presented in Section 7.

- *L. Zhou and C. Kambhamettu are with the Video/Image Modeling and Synthesis (VIMS) Lab, Department of Computer and Information Sciences, University of Delaware, Newark, DE 19716. E-mail: {lzhou, chandra}@cis.udel.edu.*
- *D. Goldgof is with the Department of Computer Science and Engineering, University of South Florida, Tampa, FL 33620. E-mail: goldgof@csee.usf.edu.*
- *K. Palaniappan is with the Multimedia Communication and Visualization Lab, Department of Computer Engineering and Computer Science, University of Missouri-Columbia, Columbia, MO 65211. E-mail: palani@cecs.missouri.edu.*
- *A.F. Hasler is with the Laboratory for Atmospheres, NASA/Goddard Space Flight Center, Greenbelt, MD 20771.*

Manuscript received 8 Mar. 2000; revised 19 Feb. 2001; accepted 6 May 2001. Recommended for acceptance by H.I. Christensen.
For information on obtaining reprints of this article, please send e-mail to: tpami@computer.org, and reference IEEECS Log Number 111670.

2 GOES Cloud Image Sequences

The current generation of Geostationary Operational Environmental Satellite (NOAA GOES 8, 9, 10) has an Imager instrument with five multispectral channels of high spatial resolution and very high dynamic range radiance measurements with 10-bit precision. In this paper, we use only the visible channel of the GOES Imager instrument that has high spatial, temporal, radiometric, and spectral resolution. The improved Imager enables more reliable automatic cloud-tracking of mesoscale atmospheric phenomena such as hurricane and severe convective storms [14], [9].

Image sequences from two satellites, GOES-8 and GOES-9, are used for the Hurricane experiments reported in this paper. During Hurricane Luis, GOES-9 collected data in Super Rapid Scan Operation mode (SRSO) in which the GOES Imager collects imagery of a fixed sector approximately once every minute and GOES-8 collected data in routine mode, which includes four US views per hour. GOES-8 was in routine mode to provide mandatory operational hemispheric coverage for other weather events that would otherwise conflict with SRSO. The subsatellite point of GOES-8 (GOES-East) is 75° W longitude, which has been remapped in our experiments to GOES-9 (GOES-West) having a subsatellite point of 135° W longitude using geolocation latitude-longitude information. Stereo analysis of these two image sequences has been done on a Maspar parallel machine, using a coarse-to-fine, hierarchical algorithm which was previously developed at NASA-Goddard [20], [9], [21]. This gives us a sequence of disparities every 15 minutes. In this work, we utilized a GOES-9 image sequence (1 frame/minute) and the available disparities (1 frame/15 minutes) to estimate dense structure, nonrigid motion, and 3D correspondences of clouds for every frame (every minute).

3 Local Motion Analysis

Cloud motion is a special case of fluid motion and consists of very complex motion dynamics. In order to obtain accurate cloud-top structure and motion, especially to capture small fluid details, local motion tracking techniques are necessary. Ideally, one would like to segment the clouds appropriately and fit different nonrigid motion models to the corresponding segmented regions. However, cloud segmentation is an extremely hard problem. In order to avoid this problem, we segment the cloud images evenly into several small regions. For each small region, if it is a small enough area, say 3×3 pixels, we can assume that this small region is undergoing nonrigid motion according to the same nonrigid motion model. Our earlier observation of cloud motion has suggested that this is a reasonable assumption for image analysis [20], [9].

An important part of local motion analysis is to define an appropriate nonrigid motion model for each local cloud region. Restricted classes of nonrigid motion, such as quasi-rigid motion, homothetic motion, or conformal motion [11], are not suitable for modeling complex cloud motion behavior. More general nonrigid motion models are desirable. In this paper, an affine motion model is used because it can be used to model general nonrigid motion and is more powerful than other restricted nonrigid motion models. The affine motion model has been experimentally confirmed as a suitable model for small local cloud motion [20], [14], [9]. In [36], we derive the relationship between the affine motion model and fluid dynamics in order to evaluate and interpret the physical model for locally affine cloud fluid motion.

Using a 3D affine motion model, we have

$$\mathbf{P}^{i+1} = \delta_i(\mathbf{M}\mathbf{P}^i + \mathbf{D}), \tag{1}$$

where $\mathbf{P}^i$ is a point in the frame i, $\mathbf{M}$ is an affine transformation matrix, and $\mathbf{D}$ is a translation vector. It can be noted that the local affine motion model is assumed to remain the same for a short period of time in (1). This is mainly due to the fact that the dual problem of structure and nonrigid motion recovery is a very ill-posed problem and it is underconstrained in terms of unknowns that need to be estimated. The above assumption will produce more constraint equations which are necessary to solve this problem. In addition, it has been experimentally proven that this assumption is valid in the local cloud motion [14], [9]. In this paper, a scaling factor δ_i is also incorporated into (1) in order to compensate for possible temporal deviations between successive cloud images. Equation (1) represents the constraint equation for tracking a point across a sequence of images using the affine motion model.

Image registration techniques (cross-correlation or optic flow) are first used to find three 2D correspondence candidates for each data point. Then, an EOF (error-of-fit) function can be defined by the sum of the minimal distance between the 2D correspondence candidates and the orthographic projection[1] of the hypothesized point obtained by (1):

$$EOF_{local1} = \sum_{i=1}^{m \text{ frames}} \sum_{j=1}^{n \text{ points}} \min\left(d_{i,j}{}^1, d_{i,j}{}^2, d_{i,j}{}^3\right), \tag{2}$$

$$d_{i,j}{}^k = \left\| \left(\delta_i \left(\mathbf{M}\mathbf{P}_{i,j} + \mathbf{D}\right)^T \mathbf{R}_{ort}\right)^T - \mathbf{C}_{i,j}{}^k \right\|, \; k = 1, 2, 3. \tag{3}$$

$\mathbf{C}_{i,j}{}^k$ are the three 2D correspondence candidates for point $\mathbf{P}_{i,j}$ and $\mathbf{R}_{ort}$ is the orthographic projection matrix. The three correspondence candidates constrain the motion to a small region in frame $i+1$ and are not used for explicitly matching feature correspondences.

The use of multiple correspondence candidates gives more flexibility to the minimization process in order to track the highly complex and dynamic cloud motion. Also, since the GOES satellite cloud images have a stereo occurrence every 15 minutes, the depth unknowns in the first frame can be eliminated by relating them to the available stereo disparities. The Levenberg-Marquardt nonlinear least-square method is utilized to solve (2) with additional depth constraints using a penalty function.

4 Global Fluid Constraints

Since the local optimization scheme performs cloud tracking within each small area independently, it suffers from discontinuities across borders as the recovered structure and motion may change a lot from one small area to the next. Also, with the absence of a global description of the cloud fluid motion, there may be a high degree of overfitting involved in the optimization of local motion model. Hence, some appropriate global constraints are necessary in order to limit possible nonrigid behaviors and regularize the locally recovered cloud motion and structure. Previous work used a hierarchical motion model with a global rigid motion to model the storm system translation and rotation [13]. In this paper, a set of global fluid constraints is incorporated using physical fluid models.

4.1 Smooth Motion Assumption

Cloud motion can be approximated as smooth deformation with local gradual variations in velocities [20], [9], This smooth motion assumption was successfully utilized for nonrigid motion recovery

1. We can consider cloud images as orthographic projections since the distance between the satellite and clouds is very large (approximately 35,787 km from mean sea level to geostationary orbit).

of 3D biomedical data [15]. In this paper, we assume that the 3D fluid flow over the entire cloud image can be approximated by a Taylor series expansion at each frame,

$$\mathbf{v}_t(\mathbf{P}) = (v_{tx}(\mathbf{P}), v_{ty}(\mathbf{P}), v_{tz}(\mathbf{P}))^T, \tag{4}$$

$$\begin{aligned} v_{tx}(\mathbf{P}) &= u_0 + u_1x + u_2y + u_3z + u_4x^2 + u_5y^2 + u_6z^2 \\ &\quad + u_7xy + u_8xz + u_9yz, \\ v_{ty}(\mathbf{P}) &= v_0 + v_1x + v_2y + v_3z + v_4x^2 + v_5y^2 + v_6z^2 \\ &\quad + v_7xy + v_8xz + v_9yz, \\ v_{tz}(\mathbf{P}) &= w_0 + w_1x + w_2y + w_3z + w_4x^2 + w_5y^2 + w_6z^2 \\ &\quad + w_7xy + w_8xz + w_9yz. \end{aligned} \tag{5}$$

Essentially, (5) assumes that the velocity components are smoothly varying functions with continuous derivatives and provides a global smoothness constraint. Many researchers have used it in fluid flow modeling and visualization. Perry and Chong [22] used it to model stationary incompressible flow fields and Ford and Strickland [4] used it for fluid flow image visualization. In our algorithm, we found that second order Taylor series expansion is a good approximation of the cloud velocity field and a smoothness force can be defined as follows, based on this observation:

$$E_{smoothness} = \sum_{i=1}^{m \text{ frames}} \sum_{j=1}^{n \text{ points}} \left\| \text{diag}\big((\mathbf{v}_{i,j} - \mathbf{v}_t^i(\mathbf{P}_{i,j}))\boldsymbol{\lambda}\big) \right\|, \tag{6}$$

$$\mathbf{v}_{i,j} = \delta^i(\mathbf{M}\mathbf{P}_{i,j} + \mathbf{D}) - \mathbf{P}_{i,j}, \tag{7}$$

where $\mathbf{v}_t^i$ is the second order Taylor series expansions defined for the velocity field in frame i and $\boldsymbol{\lambda} = (\lambda_1, \lambda_2, \lambda_3)^T$ are positive weights. Clearly, (6) can serve as an internal force which will constrain and regularize the cloud motion flow and make the motion field smooth over the entire nonrigid object (cloud). However, all the 30 coefficients in (5) are unknown initially. An approach for obtaining these coefficients will be discussed later.

4.2 Fluid Dynamics

The dynamics of fluid flows are governed by three fundamental laws: the mass conservation law, Newton's second law of motion, commonly known as Navier-Stokes equations in fluid mechanics, and the energy conservation law. Several researchers have successfully employed them in recovering 2D flows from images [31], [3], [17]. In the cloud image sequences, only kinematic information is available. So, we use only the mass conservation law to constrain the fluid cloud motion. The law of conservation of mass states that the net flux of mass entering an infinitesimal control volume is equal to rate of change of the mass of the element. For homogeneous incompressible fluid, it is the divergence-free condition,

$$\nabla \cdot \mathbf{v} = \frac{\partial v_x}{\partial x} + \frac{\partial v_y}{\partial y} + \frac{\partial v_z}{\partial z} = 0. \tag{8}$$

Since the cloud velocity components are represented by a second order Taylor series expansion, the following constraint is obtained, using conservation of mass:

$$\begin{aligned} \nabla \cdot \mathbf{v}(\mathbf{P}) &= u_1 + 2u_4x + u_7y + u_8z + v_2 + 2v_5y + v_7x \\ &\quad + v_9z + w_3 + 2w_6z + w_8x + w_9y \\ &= (u_1 + v_2 + w_3) + (2u_4 + v_7 + w_8)x \\ &\quad + (2v_5 + u_7 + w_9)y + (2w_6 + u_8 + v_9)z = 0. \end{aligned} \tag{9}$$

Equation (9) provides an additional constraint in solving for the coefficients in (5).

4.3 Incorporating the Global Constraints

A recursive algorithm is proposed to solve for the unknown coefficients in (5), incorporating the global constraints of the previous solution.

First, initial results for each small region can be obtained without global constraints by minimizing (2) locally. While the initial results may be noisy, we can use them to fit all the coefficients in (5) (velocity field function) for all the frames. The Levenberg-Marquardt method for nonlinear function optimization is used. The EOF function to fit the velocity field function in frame i can be defined as,

$$EOF^i_{global1} = \sum_{j=1}^{N \text{ points}} \left\| \mathbf{v'}_{i,j} - \mathbf{v}_t^i(\mathbf{P}_{i,j}) \right\|, \tag{10}$$

where $\mathbf{v}'_{i,j}$ is point j's velocity vector in frame i computed from the initial results. In addition, we want to include the fluid divergence-free condition (8) in the fitting procedure, which can be done by rewriting (10) as the following:

$$EOF^i_{global2} = \sum_{j=1}^{N \text{ points}} \left(\left\| \mathbf{v'}_{i,j} - \mathbf{v}_t^i(\mathbf{P}_{i,j}) \right\| + \beta \left\| (\nabla \cdot \mathbf{v}_t^i(\mathbf{P}_{i,j}) \right\| \right), \tag{11}$$

where β is a positive constant.

Second, after all the coefficients in (5) are fitted, the global constraints can be easily incorporated into the local nonrigid motion model optimization by adding the smoothness force of (6) to (2),

$$EOF_{local2} = \sum_{i=1}^{m \text{ frames}} \sum_{j=1}^{n \text{ points}} \left(\min\big(d_{i,j}{}^1, d_{i,j}{}^2, d_{i,j}{}^3\big) + cP_{i,j} \right) + E_{smoothness}, \tag{12}$$

where $P_{i,j}$ is a penalty function to enforce small changes in depth for successive frames.

Clearly, the new EOF function (12) contains both local and global information. More regularized results can be obtained by performing optimization on each small cloud region using the new EOF function. In this paper, the above procedure is performed iteratively.

The essence of this algorithm is to retrieve useful information under sufficient constraints using approximate results and then use the information as global constraints for the next iteration's optimization. In cloud motion analysis, the Taylor series coefficients represent the global flow of the cloud image and are utilized to regularize and guide the local cloud tracking. It is found that the algorithm works very well for the cloud application and the iterations achieve convergence in our experiments. Fig. 1 presents the initial results (without global constraints) and the results after seven iterations. It is clear that the initial recovered depth changes dramatically from one small region to another with a lot of noise, while the results after incorporating global constraints are very smooth.

5 Experimental Results

Our structure and motion analysis system SMAS, implemented in C (on an SGI platform), performs nonrigid motion and structure analysis on the cloud image sequences captured by GOES. To the best of our knowledge, this is the first reported system that extracts dense cloud-top heights and winds from a sequence of cloud images automatically and extends the results of [20], [9] by also recovering structure.

We have conducted our experiments on Hurricane Luis imagery, which formed as a tropical depression on 28 August 1995. After

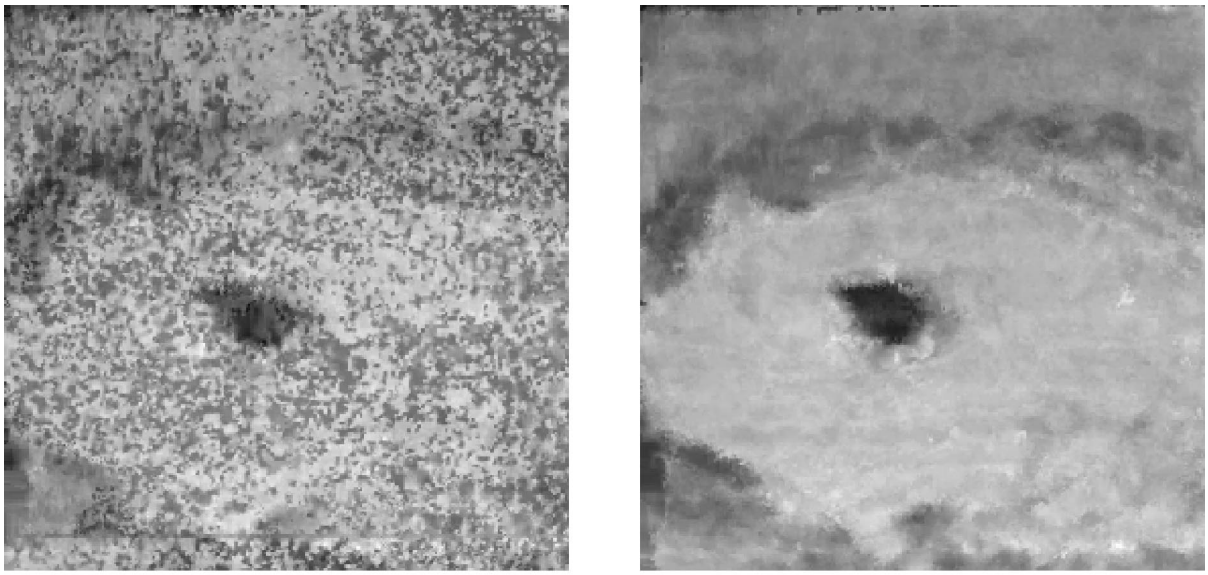

(a) (b)

Fig. 1. Comparison of the results with and without global constraints: (a) Initial results without global constraints. (b) Results after seven iterations. The 256 gray levels are rescaled from the recovered cloud depth values, which range from 0 to 16.

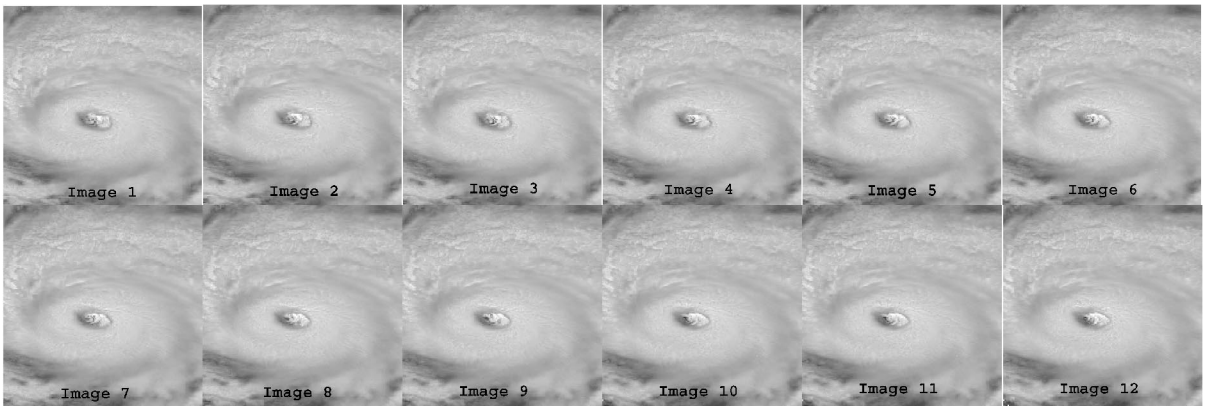

Fig. 2. Input GOES images of Hurricane Luis (from 1621 UTC to 1634 UTC).

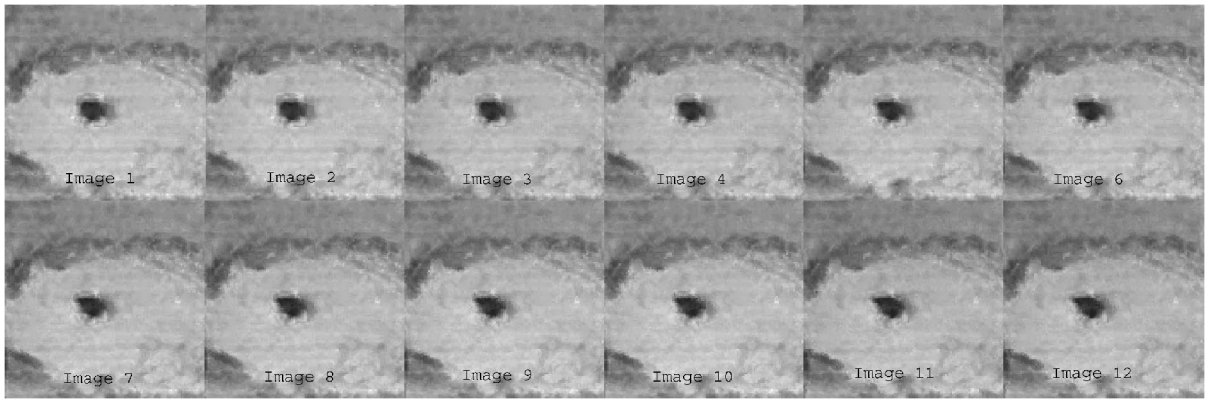

Fig. 3. Recovered cloud-top heights of Hurricane Luis (from 1621 UTC to 1634 UTC).

3.5 days as a tropical storm, it intensified to a Category 1 hurricane on 31 August and later became a Category 4 hurricane on 1 September. The track of Luis covered the outer regions of Caribbean islands, Puerto Rico, and some of the Virgin Islands. Luis did not make landfall in the US, but went back out to sea on 7 September and, by 11 September it was off the coast of Newfoundland, where it was downgraded to a Category 1 hurricane.

We present the results for a sequence of 12 hurricane Luis images (from 1621 UTC to 1634 UTC). UTC (Coordinated Universal Time) formerly known as Greenwich Mean Time (GMT) refers to the time at zero degree meridian which crosses through Greenwich, England. The first frame in the experiments starts at 1621 UTC as GOES-8 and GOES-9 images form a stereo pair at this instant. Fig. 2 shows the intensity images, from

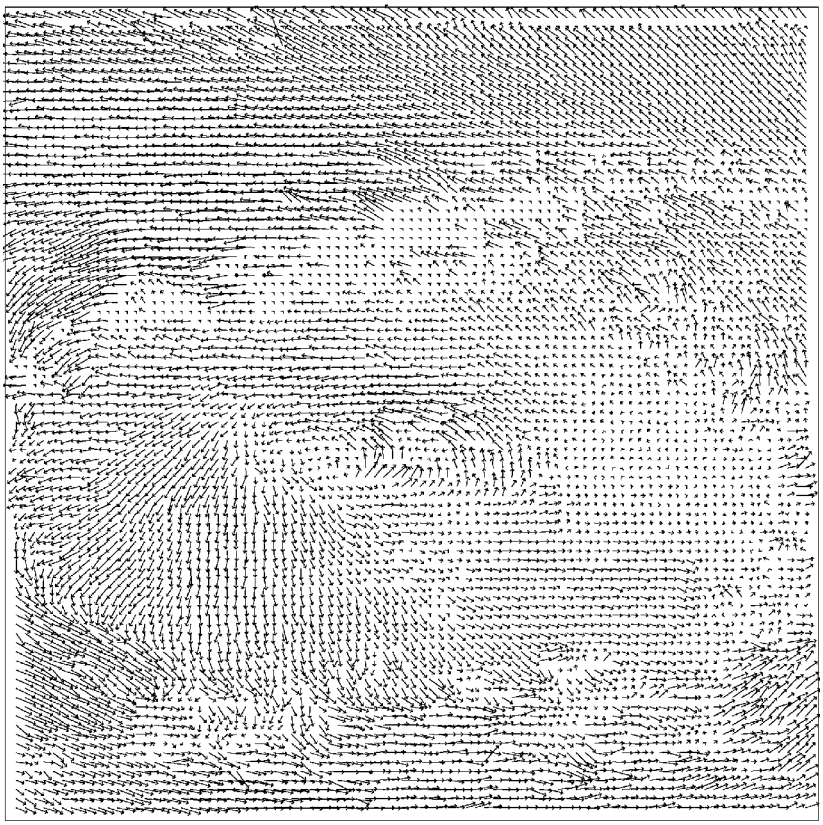

Fig. 4. Two-dimemsional projection ($x - y$ plane) of the recovered cloud motion.

1621 UTC to 1634 UTC (1-minute images from GOES-9), which are provided to our system. After seven iterations in SMAS, Fig. 3 shows the recovered dense cloud heights, which are in disparity units (pixel shifts). It was found through mathematical analysis of the position of the satellites and viewing geometry that the true cloud heights can be approximated by scaling the disparity with a constant $(height(km) = 1.78097 \times disparity)$ for midlatitude tropical storms under assumptions about atmospheric conditions [9]. In order to depict the recovered cloud motion, we visualize the cloud motion in the $x - y$ plane and in the z axis separately. In fact, due to the scaled orthographic projection of the cloud images, the recovery of z motion is very important. Fig. 4 shows the recovered cloud motion which is projected on the $x - y$ plane and Fig. 5 illustrates the recovered z direction's motion (v_z) at every iteration

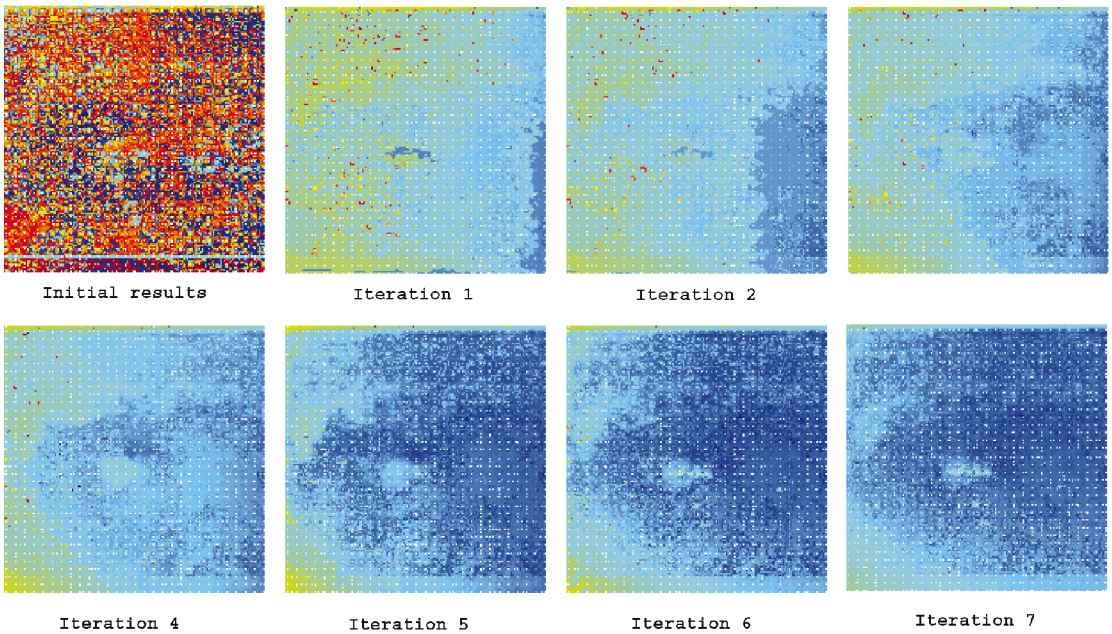

Fig. 5. Recovered cloud motion in the z direction (v_z) at every iteration step (red means v_z has a positive value whose direction is upward and blue means v_z has a negative value whose direction is downward).

TABLE 1
Comparison of the Recovered Structure and the Stereo Disparities (at UTC 1634)

	Hurricane Eye	*Hurricane Body*	*Hurricane Edge*
Mean Error (disparity)	1.037744	0.707002	1.217665

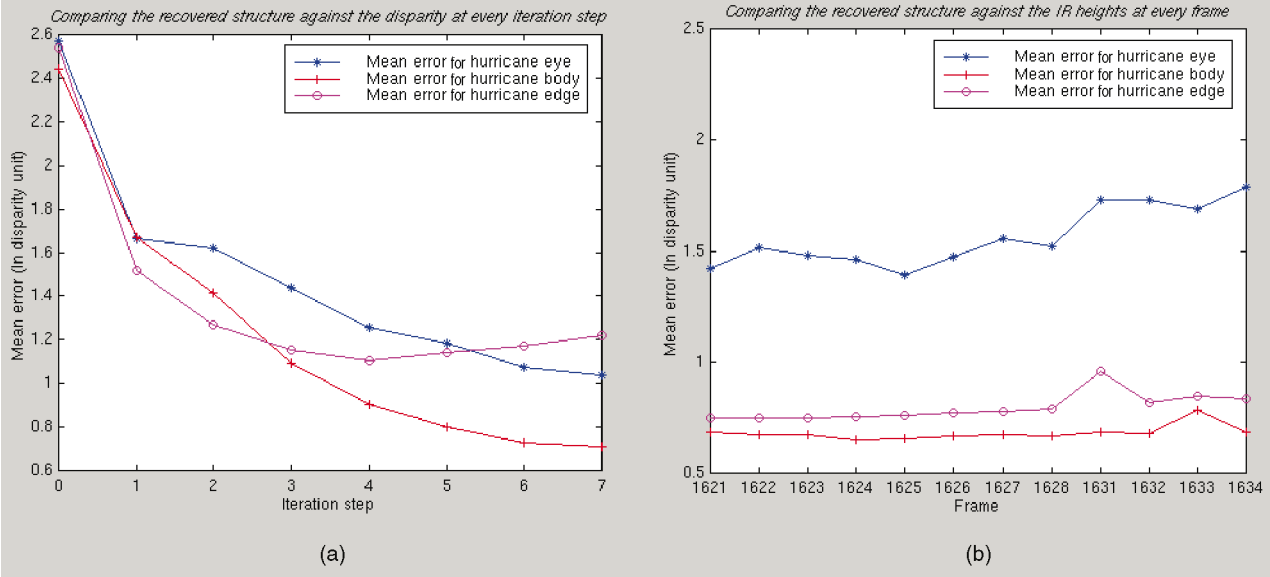

Fig. 6. (a) Comparison of the recovered structure and the stereo disparities at successive iterations. (b) Comparison of the recovered structure and the IR heights at successive frames. (The mean errors are in disparity unit.)

step in order to show the intermediate results of our algorithm. As one may expect, the initially recovered z motion is noisy. However, after the global constraints were incorporated, very good results were obtained within seven iterations. Fig. 5 shows that the final recovered cloud motion has higher v_z in the hurricane eye and lower v_z in the dense mass of high clouds forming the hurricane structure, which agrees with observations [10]. In addition, when comparing the recovered 3D cloud motion with the original images visually through animations,[2] the cloud tracking results are accurate. Close examination shows that local analysis enables our algorithm to recover different kinds of nonrigid motions locally, including cloud surface expansion, contraction, and also fluid phenomena such as cloud surface merging, splitting, and crossing over. In the following section, we further quantitatively validate our results.

6 Validations

We explore several ways of validating our results as it is difficult to get the ground truth of cloud top heights and motion. We found that our motion estimates are quite accurate when compared to manual analysis (within 1 pixel). In this section, we elaborate more on our structure estimation.

First, we compared SMAS estimated structure against the automatic stereo disparities in the last frame (UTC 1634) because UTC 1634 is the only frame (through UTC 1622 to UTC 1634) where the disparities are available. In this comparison, we found that our results are very close to the corresponding disparities for almost all the areas of the hurricane. Table 1 shows the mean errors for different parts of the hurricane. Also, we performed the same comparison at every iteration step at UTC 1634 in order to further evaluate the convergence and stability of our algorithm. Fig. 6a illustrates the change of the mean errors over successive iterations. Note that, although the initial mean errors (at iteration 0) are very large (about 2.5 disparity units), they decrease very quickly after the global constraints are applied. Stable mean errors are achieved at the seventh iteration.

Another evaluation is made by comparing the recovered cloud-top heights against the IR (infrared) temperature-based cloud-top heights. IR-based cloud heights are usually acceptable as ground-truth within high albedo dense upper clouds without thin cirrus and without significant atmospheric water vapor. Since IR heights are available at all the times, comparisons can be done for every frame (from UTC 1621 to UTC 1634) in the central dense overcast cloud regions. Fig. 6b shows the mean errors for different parts of the hurricane at every frame. It can be seen that the mean errors are consistent and negligible within the central dense overcast cloud region (hurricane body) where the IR-based heights are also most reliable.

It can also be noted that larger errors occur in the hurricane eye and the hurricane edge in both evaluations that we made. This error distribution stems from the assumption in our global constraints that clouds are homogeneous incompressible fluid. This assumption may fail in the areas of hurricane eye and hurricane edge due to the variation of cloud density and in region of high mesovortex convection such as the northwest quadrant of Hurricane Luis. Also, disparities and IR are not reliable estimates of cloud height in these areas since they are composed of multilayered thin cirrus. However, for most parts of the clouds, the mean errors are negligible (0.6 to 0.8 disparity units).

2. For more results and animations, please refer to [33].

7 Conclusions and Future Work

This paper presents the tracking of dense structure and nonrigid motion from a sequence of 2D cloud images. The main contribution of this research is that it not only deals with the problem of recovering structure from the scaled orthographic projection views but also performs nonrigid motion estimation to obtain 3D correspondences by integrating local and global analysis. The results are very encouraging and have tremendous applications in meteorology for cloud modeling and weather prediction. A similar approach can be applied for perspective projection imagery such as lip motion, human facial expressions, biomedical applications, etc.

Our future directions include the following:

1. use of complex fluid models to capture the variation of fluid density in clouds,
2. cloud motion segmentation, and
3. use of multispectral satellite images in cloud structure and nonrigid motion tracking.

Our ultimate goal is to have a set of techniques that can perform cloud motion classification and apply appropriate motion models in cloud tracking and nonrigid motion and structure analysis for long term climate studies and for short term numerical weather prediction.

Acknowledgments

Research funding was provided by US National Science Foundation Grant NSF IRI-9619240, NSF CAREER Grant IRI 998482, NSF Infrastructure Grant CISE CDA 9703088, and NASA grants NAG 5-3900, NAG 13-99014. GOES imagery was captured by the direct readout system at NASA Goddard and provided by GOES project scientist Dennis Chesters. Processing of GOES imagery for radiometric calibration, geolocation, and registration was done by Marit Jentoft-Nilsen and Hal Pierce. Insights into hurricane dynamics was provided by Peter Black at NOAA's Hurricane Research Division.

References

[1] J.K. Aggarwal and R.O. Duda, "Computer Analysis of Moving Polygonal Images," *IEEE Trans. Computers,* vol. 24, no. 10, pp. 966-976, Oct. 1975.

[2] R. Chellappa, "Structure from Motion: Light at the End of Tunnel!" *Proc. Int'l Conf. Image Processing,* p. 26PS1, 1999.

[3] E.M. Emin and P. Perez, "Fluid Motion Recovery by Coupling Dense and Parametric Vector Fields," *Proc. IEEE CS Int'l Conf. Computer Vision,* pp. 620-625, 1999.

[4] R.M. Ford and R.N. Strickland, "Representing and Visualizing Fluid-Flow Images and Velocimetry Data by Nonlinear Dynamical-Systems," *Graphical Models and Image Processing,* vol. 57, no. 6, pp. 462-482, Nov. 1995.

[5] T. Fujita, D.L. Bradbury, C. Murino, and L. Mull, "A Study of Mesoscale Cloud Motions Computed from ATS-1 and Terrestrial Photographs from Satellite," Mesometeorological Research Project Research Paper No. 71, Dept. of Geophysical Sciences, Univ. of Chicago, p. 25, 1968.

[6] A.F. Hasler, "Stereographic Observations from Satellites: An Important New Tool for the Atmospheric Sciences," *Bull. Am. Meteorological Soc.,* vol. 62, pp. 194-212, 1981.

[7] A.F. Hasler, "Stereoscopic Measurements." *Weather Satellites: Systems, Data and Environmental Applications, Section VII-3,* P.K. Rao, S.J. Holms, R.K. Anderson, J. Winston, and P. Lehr, eds., pp. 231-239, Boston: Am. Meteorlogical Soc., 1990.

[8] A.F. Hasler and K.R. Morris, "Hurricane Structure and Wind Fields from Stereoscopic and Infrared Satellite Observations and Radar Data," *J. Climate Applied Meteorology,* vol. 25, pp. 709-727, 1986.

[9] A.F. Hasler, K. Palaniappan, C. Kambhamettu, P. Black, E. Uhlhorn, and D. Chesters, "High-Resolution Wind Fields within the Inner Core and Eye of a Mature Tropical Cyclone from GOES 1-Min Images," *Bull. Am. Meteorological Soc.,* vol. 79, no. 11, pp. 2483-2496, Nov. 1998.

[10] D.P. Jorgensen, "Mesoscale and Convective-Scale Characteristics of Mature Hurricanes: Part I. General Observations by Research Aircraft," *J. Atmospheric Sciences,* vol. 41, pp. 1268-1285, 1984.

[11] C. Kambhamettu, D.B. Goldgof, D. Terzopoulos, and T.S. Huang, "Nonrigid Motion Analysis," *Handbook of Pattern Recognition and Image Processing: Computer Vision,* T. Young, ed., vol. II, pp. 405-430, San Diego, Calif.: Academic Press, 1994.

[12] C. Kambhamettu, K. Palaniappan, and A.F. Hasler, "Coupled, Multi-Resolution Stereo and Motion Analysis," *Proc. IEEE Int'l Symp. Computer Vision,* pp. 43-48, Nov. 1995.

[13] C. Kambhamettu, K. Palaniappan, and A.F. Hasler, "Hierarchical Motion Decomposition for Cloud-Tracking," *Proc. AMS 17th Conf. Interactive Information and Processing Systems (IIPS) for Meteorology, Oceanography, and Hydrology,* pp. 318-323, 2001.

[14] C. Kambhamettu, K. Palaniappan, and A.F. Hasler, "Automated Cloud-Drift Winds from GOES Images," *Proc. SPIE GOES-8 and Beyond,* vol. 2812, 122-133, Aug. 1996.

[15] C.S. Kambhamettu, "Nonrigid Motion Analysis under Small Deformations," PhD thesis, Dept. of Computer Science and Eng., Univ. of South Florida, Dec. 1994.

[16] J.A. Leese, C.S. Novak, and B.B. Clark, "An Automated Technique for Obtaining Cloud Motion from Geosynchronous Satellite Data Using Cross-Correlation," *J. Applied Meteorology,* vol. 10, pp. 118-132, 1971.

[17] M. Maurizot, P. Bouthemy, and B. Delyon, "2D Fluid Motion Analysis from a Single Image," *Proc. IEEE Conf. Computer Vision and Pattern Recognition,* pp. 184-191, 1998.

[18] P. Minnis, P.W. Heck, and E.F. Harrison, "The 27-28 October 1986 Fire IFO Cirrus Case Study: Cloud Parameter Fields Derived from Satellite Data," *Monthly Weather Rev.,* vol. 118, pp. 2426-2447, 1990.

[19] K. Palaniappan, M. Faisal, C. Kambhamettu, and A.F. Hasler, "Implementation of an Automatic Semi-Fluid Motion Analysis Algorithm on a Massively Parallel Computer," *Proc. IEEE Int'l Parallel Processing Symp.,* pp. 864-872, 1996.

[20] K. Palaniappan, C. Kambhamettu, A.F. Hasler, and D.B. Goldgof, "Structure and Semi-Fluid Motion Analysis of Stereoscopic Satellite Images for Cloud Tracking," *Proc. Int'l Conf. Computer Vision,* pp. 659-665, 1995.

[21] K. Palaniappan, J. Vass, and X. Zhuang, "Parallel Robust Relaxation Algorithm for Automatic Stereo Analysis," *Proc. SPIE Parallel and Distributed Methods for Image Processing II,* pp. 958-962, 1998.

[22] A.E. Perry and M.S. Chong, "A Description of Eddying Motions and Flow Patterns Using Critical Point Concepts," *Ann. Rev. Fluid Mechanics,* vol. 19, pp. 125-155, 1987.

[23] D.R. Phillips, E.A. Smith, and V.E. Suomi, "Comment on 'An Automated Technique for Obtaining Cloud Motion from Geosynchronous Satellite Data Using Cross-Correlation,' *J. Applied Meteorology,* vol. 11, pp. 752-754, 1972.

[24] A.F. Hasler, R.A. Mack, and R.F. Adler, "Thunderstorm Cloud Top Observations Using Satellite Stereoscopy," *Monthly Weather Rev.,* vol. 111, pp. 1949-1964, 1983.

[25] E. Rodgers, R. Mack, and A.F. Hasler, "A Satellite Stereoscopic Technique to Estimate Tropical Cyclone Intensity," *Monthly Weather Rev.,* vol. 111, pp. 1599-1610, 1983.

[26] E.A. Smith and D.R. Phillips, "Automated Cloud Tracking Using Precisely Aligned Digital ATS Pictures," *IEEE Trans. Computers,* vol. 21, pp. 715-729, 1972.

[27] C.S. Velden, "Winds Derived from Geostationary Satellite Moisture Channel Observations: Applications and Impact on Numerical Weather Prediction," *Meteorology and Atmospheric Physics,* vol. 60, pp. 37-46, 1996.

[28] C.S. Velden, C.M. Hayden, S. Nieman, W.P. Menzel, S. Wanzong, and J. Goerss, "Upper-Tropospheric Winds Derived from Geostationary Satellite Water Vapor Observations," *Am. Meteorological Soc.,* vol. 78, pp. 173-195, 1997.

[29] C.S. Velden, T.L. Olander, and S. Wanzong, "The Impact of Multispectral GOES-8 Wind Information on Atlantic Tropical Cyclone Track Forecasts in 1995. Part 1: Dataset Methodology, Description and Case Analysis," *Monthly Weather Rev.,* 1998.

[30] J. Weng, N. Ahuja, and T.S. Huang, "3D Motion Estimation, Understanding and Prediction from Noisy Image Sequences," *IEEE Trans. Pattern Analysis and Machine Intelligence,* vol. 9, pp. 370-389, 1987.

[31] R.P. Wildes, M.J. Amabile, A.M. Lanzillotto, and T.S. Leu, "Recovering Estimates of Fluid Flow from Image Sequence Data," *Computer Vision and Image Understanding,* vol. 80, no. 2, pp. 246-266, Nov. 2000.

[32] G.S. Young and R. Chellappa, "3D Motion Estimation Using a Sequence of Noisy Stereo Images: Models, Estimation, and Uniqueness Results," *IEEE Trans. Pattern Analysis and Machine Intelligence,* vol. 12, no. 8, pp. 735-759, Aug. 1990.

[33] L. Zhou and C. Kambhamettu http://www.cis.udel.edu/~vims, 2001.

[34] L. Zhou, C. Kambhamettu, and D.B. Goldgof, "Structure and Nonrigid Motion Analysis of Satellite Cloud Images," *Proc. Indian Conf. Computer Vision, Graphics, and Image Processing,* pp. 285-291, Dec. 1998.

[35] L. Zhou, C. Kambhamettu, and D.B. Goldgof, "Extracting Nonrigid Motion and 3D Structure of Hurricanes from Satellite Image Sequences without Correspondences," *Computer Vision and Pattern Recognition,* vol. ll, pp. 280-285, 1999.

[36] L. Zhou, "3D Nonrigid Motion Analysis from 2D Images," PhD thesis, Dept. of Computer and Information Sciences, Univ. of Delaware, Feb. 2001.